

UCLA

UCLA Previously Published Works

Title

Functional organization of the insula in men and women with obstructive sleep apnea during Valsalva.

Permalink

<https://escholarship.org/uc/item/5ff4t8pc>

Journal

Sleep, 44(1)

ISSN

0161-8105

Authors

Pal, Amrita
Ogren, Jennifer A
Aguila, Andrea P
et al.

Publication Date

2021-01-21

DOI


10.1093/sleep/zsaa124

Peer reviewed



ORIGINAL ARTICLE

Functional organization of the insula in men and women with obstructive sleep apnea during Valsalva

Amrita Pal¹, Jennifer A. Ogren², Andrea P. Aguila¹, Ravi Aysola³,
Rajesh Kumar^{4,5}, Luke A. Henderson⁶, Ronald M. Harper² and
Paul M. Macey^{1,*}

¹UCLA School of Nursing, University of California, Los Angeles, CA, ²Department of Neurobiology, David Geffen School of Medicine at UCLA, University of California, Los Angeles, CA, ³Division of Pulmonary and Critical Care, David Geffen School of Medicine at UCLA, University of California, Los Angeles, CA, ⁴Department of Anesthesiology, David Geffen School of Medicine at UCLA, University of California, Los Angeles, CA, ⁵Department of Radiological Sciences, David Geffen School of Medicine at UCLA, University of California, Los Angeles, CA and ⁶Department of Anatomy and Histology, Sydney Medical School, University of Sydney, Sydney, Australia

*Corresponding author. Paul M. Macey, UCLA School of Nursing, 700 Tiverton Ave, Los Angeles, CA 90095-1702. Email: pmacey@ucla.edu.

Abstract

Study Objectives: Obstructive sleep apnea (OSA) patients show impaired autonomic regulation, perhaps related to functional reorganization of the insula, which in healthy individuals shows sex-specific anterior and right dominance during sympathetic activation. We examined insular organization of responses to a Valsalva maneuver in OSA with functional magnetic resonance imaging (fMRI).

Methods: We studied 43 newly diagnosed OSA (age mean \pm SD: 46.8 \pm 8.7 years; apnea-hypopnea index (AHI) \pm SD: 32.1 \pm 20.1 events/hour; 34 males) and 63 healthy (47.2 \pm 8.8 years; 40 males) participants. Participants performed four 18-second Valsalva maneuvers (1-minute intervals, pressure \geq 30 mmHg) during scanning. fMRI time trends from five insular gyri—anterior short (ASG); mid short (MSG); posterior short (PSG); anterior long (ALG); and posterior long (PLG)—were assessed for within-group responses and between-group differences with repeated measures ANOVA ($p < 0.05$); age and resting heart rate (HR) influences were also assessed.

Results: Right and anterior fMRI signal dominance appeared in OSA and controls, with no between-group differences. Separation by sex revealed group differences. Left ASG anterior signal dominance was lower in OSA versus control males. Left ASG and ALG anterior dominance was higher in OSA versus control females. In all right gyri, only OSA females showed greater anterior dominance than controls. Right dominance was apparent in PSG and ALG in all groups; females showed right dominance in MSG and PLG. OSA males did not show PLG right dominance. Responses were influenced substantially by HR but modestly by age.

Conclusions: Anterior and right insular fMRI dominance appears similar in OSA versus control participants during the sympathetic phase of the Valsalva maneuver. OSA and control similarities were present in just males, but not necessarily females, which may reflect sex-specific neural injury.

Statement of Significance

The left and right insular cortices are brain regions that coordinate cardiovascular responses to blood pressure changes, which, since damaged in obstructive sleep apnea (OSA), may contribute to the autonomic disruptions in the sleep disorder. We studied the functional organization of the insular cortices in OSA and healthy participants with functional magnetic resonance imaging (fMRI) during Valsalva challenges, and found OSA patients showed similar response patterns as healthy participants, namely right and anterior dominance of responses during the sympathetic phase. Separating by sex confirmed the findings in males, but a small sample of females showed greater anterior activation of the right insula in OSA compared with healthy participants. These findings suggest insular organization of autonomic responses is intact in males with OSA, and there may be female-specific disruption possibly related to female-specific brain injury.

Key words: fMRI; autonomic nervous system; blood pressure

Submitted: 24 February, 2020; Revised: 11 May, 2020

© Sleep Research Society 2020. Published by Oxford University Press on behalf of the Sleep Research Society. All rights reserved. For permissions, please e-mail journals.permissions@oup.com.

Introduction

Obstructive sleep apnea (OSA) occurs in over 30% of men and 15% of women, and is a strong risk factor for cardiovascular disease [1, 2]. A major concern for the field is that the principal intervention, continuous positive airway pressure (CPAP) [3], is insufficient to address the risk of comorbid cardiovascular issues, notably hypertension [4, 5]. Although hypertension is the number one comorbidity of OSA, in practice, CPAP has only a modest impact on lowering blood pressure (BP) [1, 6, 7]. There is debate whether the existing evidence reflects limited benefits of CPAP versus study design confounds related to compliance or participant selection [8–10], with a 2016 clinical trial reporting no benefit on cardiovascular risk reduction, eliciting substantial commentary [4]. Multiple findings of CPAP improving autonomic markers to some degree exist in some populations (e.g. [11, 12]). Nevertheless, the absence of consistent CPAP findings leaves open the question of what are possible contributors to high BP in OSA.

The variability in CPAP/OSA-related hypertension outcomes may stem from underlying brain injury accompanying OSA, and related impaired autonomic nervous system regulation; some injury is, at least in part, not readily recoverable [13]. The impaired autonomic action is both sustained, likely resulting from high sympathetic tone and expressed as hypertension [14], and transient, as reflected in challenges resulting in impaired acute heart rate (HR) and BP responses to physical stimuli [15, 16]. Medullary structures that regulate sympathetic output from the spinal cord to the vasculature and heart receive modulating influences from an array of suprapontine and cerebellar structures, which include the ventromedial and dorsolateral frontal, cingulate, and insular cortices [17–25]. Many of those areas are injured in OSA, especially the cerebellum and the insular cortex, the latter showing both altered anatomy and abnormal activity to autonomic challenges [13, 26–34]. The bilateral insulae are large nonhomogenous cortical areas with separate gyri displaying differential functions with respect to the autonomic control [35, 36]. Five major gyri (anterior short gyrus [ASG], middle short gyrus [MSG], and posterior short gyrus [PSG] anteriorly; and anterior long gyrus [ALG] and posterior long gyrus [PLG] posteriorly) serve different roles during sympathetic activation [36–38]. In healthy participants, greater neural activity during sympathetic challenges appears in the right anterior insula relative to the left posterior insula [35, 36]. Electrical stimulation of the left insula in humans evokes decreased HR and BP, while right-side stimulation evokes increases, and damage by strokes in the right insula causes greater cardiovascular dysregulation than those affecting the left [39, 40].

The major influences of the insular cortices on normal autonomic regulation suggest a significant role in disrupted control by those structures in OSA, i.e. the persistent high BP dysfunctional responses to cardiovascular challenges in OSA, even following CPAP therapy [36]. Sex differences are apparent in both autonomic regulation by the insula [38, 41] and in OSA-related brain injury [42–44]. Clinical cardiovascular characteristics of OSA also vary by sex, such as morning BP patterns [45] and responses to acute BP challenges [15], raising the possibility that OSA-related influences on insular functional organization differ by sex. The objective here was to determine the nature of insular functional organization during an autonomic challenge in OSA to gain insights into insular contributions to the impaired cardiovascular responses in the breathing disorder, with secondary

consideration of sex. We earlier showed roles of anterior gyri and right-sided dominance in control participants [36, 38] during Valsalva maneuvers (exhalation against a closed glottis) which evoke sympathetic and parasympathetic responses [46, 47]. We hypothesized that functional insular organization to this autonomic challenge task would be altered in OSA in a sex-specific manner; specifically, that functional magnetic resonance imaging (fMRI) patterns would parallel the delayed and muted cardiovascular responses found earlier [15]. We previously published detail analyses of cardiovascular and cerebral blood flow influences in OSA [15, 48], so for the present study, we focused on neural function using fMRI data from those same experiments. We assessed OSA and control as groups with combined sexes, and males and females separately as secondary analyses, although the study was not originally powered to be sex-specific. The outcomes have the potential to contribute to insights on sex-based differences in cardiovascular consequences of OSA, and to focus on interventional processes to enhance or replace positive pressure treatments for the condition.

Methods

Participants

We studied 106 people, including 43 newly diagnosed, untreated OSA patients (34 males, 9 females) and 63 healthy control participants (43 males, 23 females); details are in Table 1. OSA patients were recruited from the UCLA Sleep Disorders Center. All OSA patients were diagnosed with OSA according to the 1999 American Academy of Sleep Medicine guidelines [49]. All control participants were screened for OSA using a semistructured interview to assess daytime sleepiness, snoring, bed partner report of breathing difficulties during sleep, and nighttime gasping episodes, and referred to a full sleep study if those symptoms were present. Exclusion criteria for all participants included other sleep disorders, major illness or head injury, stroke, major cardiovascular disease, current use of psychotropic or cardiovascular medications other than statins, and diagnosed mental disorder. The procedures were approved by the UCLA Institutional Review Board, and all participants provided written, informed consent.

Measurements

Brain blood-oxygen-level-dependent (BOLD) fMRI signals were recorded in a 3.0 Tesla Siemens Trio MRI scanner with an 8-channel head coil. We used a standard echo-planar imaging protocol (repetition time [TR] = 2000 ms; echo time [TE] = 30 ms; flip angle = 90°; matrix size = 64 × 64; field of view = 230 mm × 230 mm; slice thickness = 4.5 mm). A pulse oximeter (Nonin 8600FO) with a sensor on the left index finger was used to assess physiology, and the plethysmographic waveform (SaO₂) was recorded at 1 kHz. For spatial localization, two high-resolution, T1-weighted anatomical images were acquired with a magnetization-prepared rapid acquisition gradient echo sequence (TR = 2200 ms; TE = 2.2 ms; inversion time = 900 ms; flip angle = 9°; matrix size = 256 × 256; field of view = 230 × 230 mm; slice thickness = 1.0 mm). These two scans were realigned and averaged for each participant to result in one anatomical reference.

Table 1. Participant information

	All			Male			Female		
	CONTROL Mean \pm SD [range] N = 63	OSA Mean \pm SD [range] N = 43	<i>p</i> [†] OSA vs. CONTROL	CONTROL Mean \pm SD [range] N = 40	OSA Mean \pm SD [range] N = 34	<i>p</i> [†] OSA vs. CONTROL	CONTROL Mean \pm SD [range] N = 23	OSA Mean \pm SD [range] N = 9	<i>p</i> [†] OSA vs. CONTROL
Age (years)	47.2 \pm 8.8 [30.9–65.8]	46.8 \pm 8.73 [30.9–62.7]	0.69	45.9 \pm 9.1 [30.9–64.5]	45.5 \pm 8.8 [30.85–62.84]	0.86	50.3 \pm 7.8 [40.25–65.8]	51.7 \pm 6.8 [37.29–59.4]	0.65
BMI (kg/m ²)	24.7 \pm 3.8 [16.6–35.5]	30.4 \pm 4.7 [21.5–43.2]	<0.001	25.2 \pm 2.8 [17.7–29.8]	29.8 \pm 4.8 [21.5–43.2]	<0.001	23.9 \pm 5.0 [16.6–35.5]	32.6 \pm 3.9 [26.4–37.6]	<0.001
Resting HR (bpm)	73.1 \pm 14.2 [49–120]	72.8 \pm 10.9 [49–95]	0.91	70.5 \pm 13.3 [49–120]	74.3 \pm 11.1 [49–95]	0.19	77.6 \pm 14.7 [58–115]	67.0 \pm 8.1 [52–77]	0.05
Sleep parameters for OSA									
AHI (events/ hour)	n/a	32.1 \pm 20.1 [5–100.7]	n/a	n/a	35.1 \pm 20.2 [10–100.7]	n/a	n/a	20.6 \pm 16.3 [5–58.3]	n/a
SaO ₂ (minimum %)	n/a	80.0 \pm 9.7 [50–96]	n/a	n/a	77.5 \pm 9.1 [50–95]	n/a	n/a	87.3 \pm 5.5 [80–96]	n/a
SaO ₂ (baseline %)	n/a	94.8 \pm 2.0 [88–97]	n/a	n/a	94.9 \pm 2.1 [88–97]	n/a	n/a	94.8 \pm 1.6 [92–97]	n/a

Characteristics of OSA and control groups, with separation by sex. Group differences were tested with two-way ANOVA for OSA parameters, *p*-values have been indicated (italicized if ≤ 0.05).

[†]*p* for two-way ANOVA *F*-test, group comparison OSA vs. CONTROL.

Protocol

Participants were asked to refrain from coffee and other substances with stimulants for 24 hours prior to the study. While lying in a scanner, following a 1-minute baseline, participants performed four 18-second Valsalva maneuvers at 1-minute intervals against a closed glottis. Timing was synchronized to the fMRI scans. A target expiratory pressure of 30 mmHg was set, which normally elicits sympathetic and parasympathetic responses as well as BP and HR changes. The target pressure was measured via tubing connected to a pressure sensor, and a light signal turned on to indicate the target was reached. All participants included in the analysis maintained target pressures for all four challenges (one female OSA patient who did not was excluded). Scanning continued until 1 minute after the fourth Valsalva.

Analysis: physiology and participant characteristics

We measured HR from the SaO₂ signal using peak detection. The median HR was calculated over the 60-second baseline period immediately prior to the first Valsalva. The age, body mass index (BMI), and HR, and sleep parameters for the patient group, were described and compared between OSA and control groups using an ANOVA model. The full assessment of beat-to-beat HR responses was presented earlier [15].

Analysis: MRI

We preprocessed the fMRI scans using SPM12 (<https://www.fil.ion.ucl.ac.uk/spm>). Images were realigned for motion correction, and linear detrended over each series. For each participant, scans were spatially normalized in two steps, first coregistering the mean fMRI to the T1 anatomical scan and then warping to the “vbm8” template in Montreal Neurological Institute (MNI) space based on the T1 “DARTEL” spatial normalization algorithm [50].

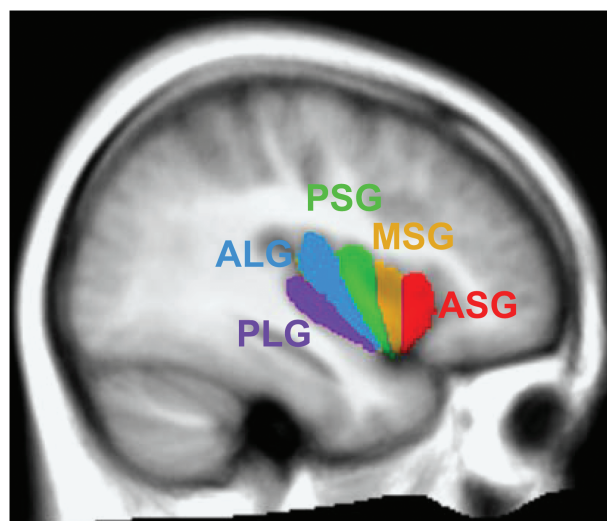


Figure 1. Insular gyri. Illustration of insular gyri overlaid onto average of all participants' anatomical scans. From anterior to posterior organization: ASG (anterior short gyrus), MSG (middle short gyrus), PSG (posterior short gyrus), ALG (anterior long gyrus), PLG (posterior long gyrus).

The five major gyri were parcellated from the average of the high-resolution T1-weighted scans: three short (anterior) gyri and two long (posterior) gyri: ASG, MSG, PSG, ALG, and PLG as represented in Figure 1. Two experienced research team members determined the parcellation based on manual tracing with reference to a brain atlas [51]. The regions were outlined in normalized space; although this approach is slightly less accurate than individual tracing, the resolution of the fMRI data ($>50 \text{ mm}^3$) relative to the anatomical scans ($<1 \text{ mm}^3$) is such that any differences in accuracy would not be meaningful. Signal intensity changes over time were extracted from each voxel in each gyrus from the processed images. For each gyrus in each participant, a mean time trend over all voxels was then calculated. Time trends were converted to percent change relative to

the mean of the 1-minute baseline period. For each participant, the signals from the four challenges were separate and averaged to create one single Valsalva percent change time trend that was passed to the group level analysis. While this averaging could theoretically result in reduced sensitivity, in practice the statistical approach we chose takes advantage of repeated measures, and could detect small effect sizes.

To assess posterior–anterior effects, signal intensity changes were calculated relative to those in the PLG. As discussed above, the importance of the anterior insula has been observed in clinical and animal studies. Our previous work showed this anterior-specific role could be demonstrated by comparing the fMRI signal in the anterior- versus posteriormost insula (PLG), so we repeated this technique here [36]. At each time point, signal intensity changes within the PLG were subtracted from those in the ASG, MSG, PSG, and ALG for each hemisphere so that direct comparisons between these regions and the PLG could be assessed. Lateralization was assessed by subtracting signal changes in each of the five left gyri from the corresponding gyri on the right side; for example, ASG laterality was calculated by subtracting the left ASG time trend from the right ASG time trend.

The resulting fMRI signals were assessed for within- and between-group differences using repeated measures ANOVA (RMANOVA). The analysis was implemented with SAS “proc mixed,” as described earlier [52, 53]. In brief, this approach

assesses within-group changes and between-group differences over time, with each 2-second time point during and after the challenge assessed relative to baseline time points. We applied the Tukey–Fisher criterion for multiple comparisons; that is, we assessed the overall model for significance ($p \leq 0.05$), and then effects of interest (time, group by time), before considering individual time points of difference. The latter tests are performed within the “proc mixed” procedure, as the output includes time-point tests of significance (hence, no post hoc tests were needed). We assessed the effects in combined and sex-specific models.

The RMANOVA mixed model approach allows for continuous variables to be included, so we performed secondary analyses of age and resting HR. We created four models that included different age effects added to the main model (group + time + group × time):

- 1) Main + age: age effects independent of group over the entire protocol, independent of time;
- 2) Main + age + age × group: group-specific effects of age over the entire protocol, independent of time;
- 3) Main + age + age × time: age effects on Valsalva responses, independent of group;
- 4) Main + age + age × group + age × time + age × group × time: age effects on between-group differences in Valsalva responses.

Table 2. Intrinsic PLG changes in the left and right insula

Model details		All		Male		Female	
		Left PLG	Right PLG	Left PLG	Right PLG	Left PLG	Right PLG
Main model: group, time group, time	Significance as χ^2 (all $p < 0.0001$)	186.96	129.68	124.6	85.95	67.47	64.98
	Fit ($-2 \log$ -likelihood)	24 142.6	24 156.7	16 994.3	17 055.5	6958.7	6885
	Group effect p -value (mean over entire series for each group)	0.11	0.05	0.89	0.51	0.03	0.04
Valsalva response: within-group	Time (within-group effect of time) p -values						
	Main	<0.001	<0.001	<0.001	<0.001	<0.001	<0.001
	Main + Age	<0.001	<0.001	<0.001	<0.001	<0.001	<0.001
	Age × Group	<0.001	<0.001	<0.001	<0.001	<0.001	<0.001
	Age × Time	0.046	0.29	0.51	0.84	0.001	<0.001
	Age × Group × Time	0.046	0.29	0.51	0.84	0.001	<0.001
	HR	<0.001	<0.001	<0.001	<0.001	<0.001	<0.001
	HR × Group	<0.001	<0.001	<0.001	<0.001	<0.001	<0.001
	HR × Time	0.98	0.96	0.96	0.79	0.24	0.62
Valsalva response: between-group	Time × Group (between-group effect of time) p -values						
	Main	0.21	0.03	0.45	0.32	<0.01	<0.01
	Age	0.21	0.03	0.45	0.32	<0.01	<0.01
	Age × Group	0.21	0.03	0.45	0.32	<0.01	<0.01
	Age × Time	0.21	0.03	0.45	0.31	0.001	0.001
	Age × Group × Time	0.21	0.03	0.45	0.31	0.001	0.001
	HR	0.21	0.03	0.45	0.32	<0.01	<0.01
	HR × Group	0.21	0.03	0.45	0.32	<0.01	<0.01
	HR × Time	0.21	0.03	0.46	0.47	0.14	0.1
	HR × Group × Time	0.21	0.03	0.46	0.47	0.14	0.1

The model fit is indicated by $-2 \times \log$ -likelihood as calculated by SAS (higher indicates better fit). The p -value variables in models are reported (italicized if ≤ 0.05). This table presents salient statistics from nine RMANOVA models for left and right PLG in three sets (mixed, male, female). Full data are available online [54]. The main model (bold) is the interaction of group-by-time (fMRI = group + time + group × time), and measures of significance and fit are in the top rows of the table. The “Group” effect is the mean over the entire series and does not represent responses, and is not discussed. The two effects of interest “Time,” which represents within-group responses over time, and “Time × Group,” which represents between-group differences in responses. The p -values for these effects are shown for the nine models. All models include the main effects plus additional mean or interaction terms. All interaction models also include means. For example, “Age × Time” is fMRI = group + time + group × time + age + age × time.

We repeated these for models with HR in place of age. For the purposes of this study, we only focused on the within and between OSA and control group responses in the different models. The age-by-time and HR-by-time are not independent of the main effects of interest, but nevertheless the degree to which these secondary models affect the within- and between-group *p*-values will reflect potential associations between the clinical and fMRI measures.

Results

Participants

Table 1 shows participant characteristics. Age was similar between OSA and control groups, and as expected, BMI was high in OSA. HR was lower in female OSA compared with female control participants. Our earlier study showed the impaired beat-by-beat HR responses; the prior study also showed no group differences between Valsalva pressures [15].

Intrinsic PLG changes in left and right insula

Table 2 and Figure 2 show the left and right insula intrinsic PLG responses. The responses mostly occurred during phase II of the Valsalva (last 12–16 seconds of the exhale period), the most sympathetically dominant period. While other time points in phase IV (6+ seconds after end of exhale) also showed statistically significant within- and between-group responses, the effect sizes were much smaller than during phase II. Females but not males showed significant OSA versus control differences in the

left and right PLG. Both within- and between-group differences in response were influenced by resting HR but not age (Table 1).

Left side anterior–posterior organization

Figure 3 represents the left insula anterior-to-posterior functional organization during Valsalva maneuvers, with positive values representing greater anterior dominance. Table 3 shows the model statistics. The mean \pm SEM percentage change fMRI signal for each of left ASG, MSG, PSG, and ALG with respect to PLG is shown for all participants, and separately for males and females. For example, signal intensity in the left ASG, changes during Valsalva maneuvers were approximately 1% higher relative to those changes in the left PLG in both control and OSA groups. The overall model statistics in Table 3 show that no between-group differences appeared in the combined groups for the left ASG, MSG, PSG, or ALG. However, separation by sex showed OSA-related effects in males in the ASG, with lower dominance in the OSA group than the control group. No differences between controls and OSA male participants occurred in the other three left gyri. In contrast, OSA females showed greater anterior dominance in the ASG than controls. OSA also exerted an effect in females in the ALG, with the control group showing PLG dominance, but little effect in the OSA group. Within-group effects, i.e. OSA and control responses during the Valsalva and recovery, showed mostly anterior dominance in the short gyri. The ALG showed little or no dominance in most groups. The influence of age or HR on the main effects was noted where *p*-values changed substantially. Age had no influence on any within- or between-group effects. The interaction of baseline HR and time (meaning HR influence on Valsalva responses)

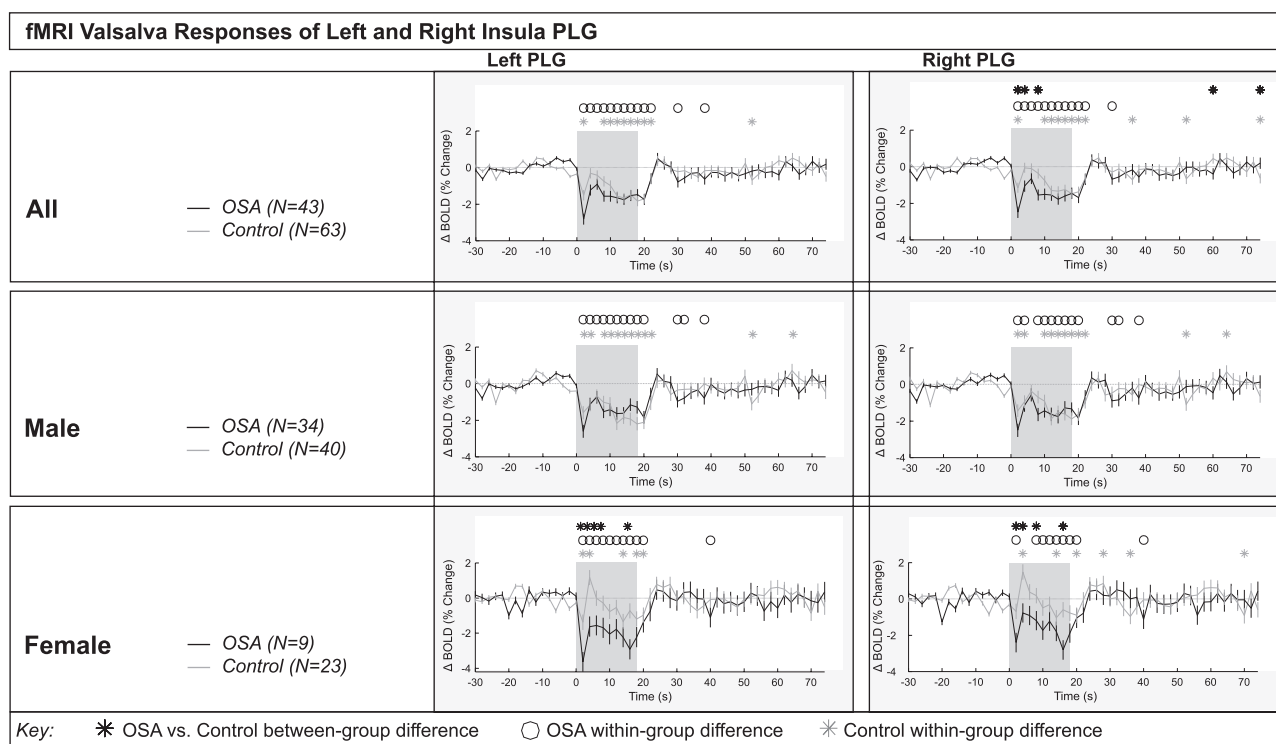


Figure 2. PLG intrinsic changes in left and right insula. Left and right hemisphere fMRI signals of PLG for combined (top panel), males (middle panel), and females (bottom panel). The graphs reflect % change relative to baseline (group mean \pm SE), averaged over four challenges, with time points of significant increase or decrease relative to baseline within-group, and time points of between-group differences (RMANOVA, $p \leq 0.05$).

influenced within-group effects for all groups in the ASG and MSG, and between-group effects in females in the ASG and ALG.

Right side anterior-posterior organization

Figure 4 represents the right insula anterior-to-posterior functional organization during Valsalva maneuvers, with positive values representing greater anterior dominance. Table 4 shows the model statistics. The percentage change fMRI signal for each of right ASG, MSG, PSG, and ALG with respect to right PLG is shown for all participants, and separately for males and females. Similar to the left side, while signal intensity during a Valsalva was greater in right ASG, MSG, and PSG relative to the right PLG, there were no significant differences between the control and OSA groups; Table 4 shows that no between-group differences appeared in the combined groups. However, as with the left side, significant differences occurred when participants were separated by sex. Again, females in the OSA group displayed greater relative signal intensity changes during Valsalva than controls in the right ASG, MSG, PSG, and ALG. No significant differences occurred in the male group for any of the gyri. Additionally, within-group

effects, meaning OSA and control responses during the Valsalva and recovery, were similar to the left insula, with mostly anterior dominance in the short gyri. The ALG showed little or no dominance in most groups. The interaction of age by time (meaning age influences on Valsalva responses) affected all within-group effects, but age had no influence on any between-group effects. The interaction of baseline HR and time (meaning HR influence on Valsalva responses) influenced within-group effects for females in the MSG, PSG, and ALG. Between-group effects were influenced in females by all HR models in all gyri.

Laterality

Figure 5 shows the laterality of the insula responses during the Valsalva maneuver, with positive values reflecting right dominance. Table 5 shows the model statistics. The right-minus-left percentage change fMRI signal for each gyrus is shown for all participants, and separately for males and females. In the combined participants, there was no group difference in the response of the right compared with the left during the Valsalva for any insula gyri. That is, the overall model statistics

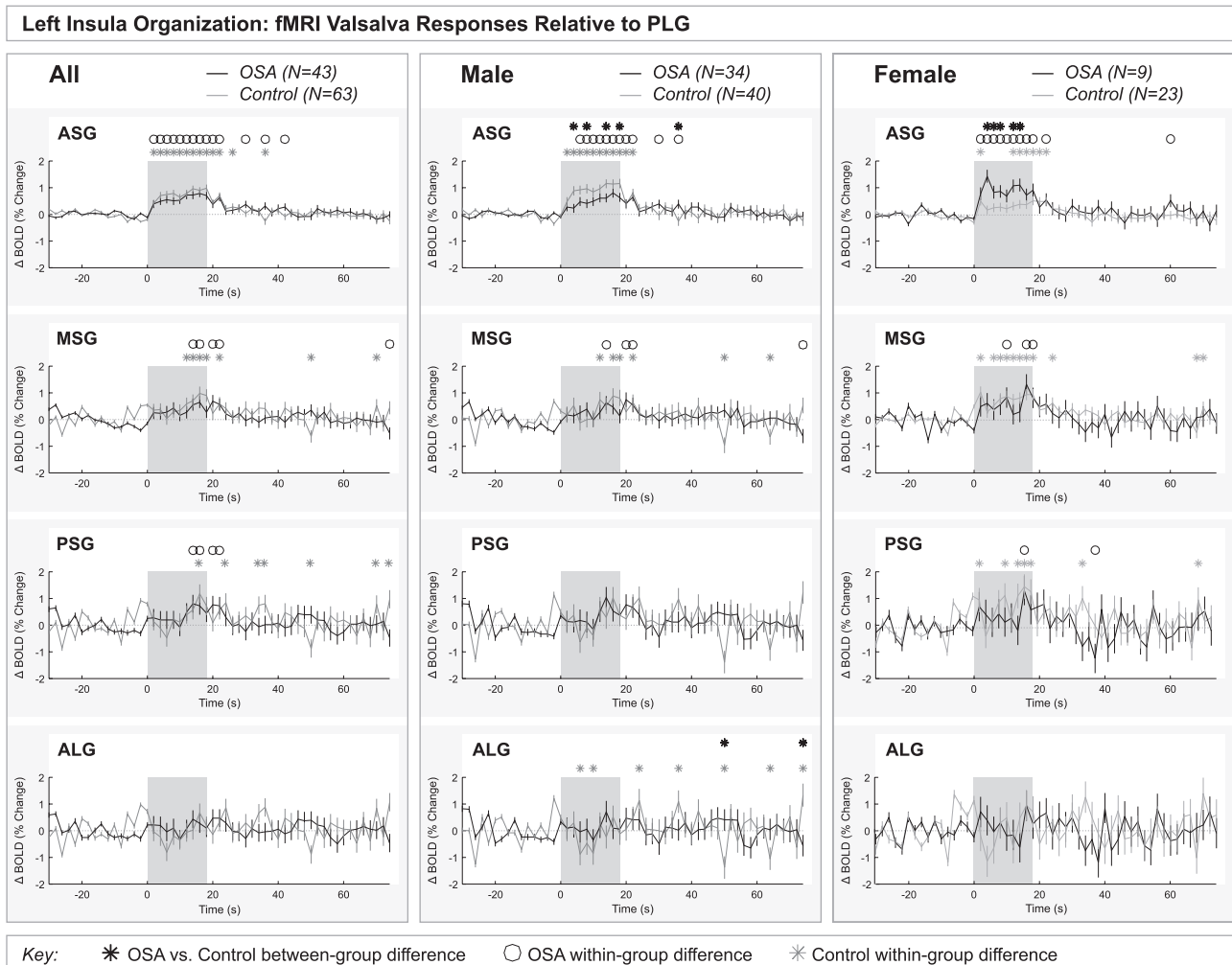


Figure 3. Anterior-posterior organization of left insula. Left hemisphere fMRI signals relative to PLG such that positive change reflects anterior dominance. Baseline (group mean ± SE), averaged over four challenges, with time points of significant increase or decrease relative to baseline within-group, and time points of between-group differences (RMANOVA, $p \leq 0.05$) for the anterior-posterior responses by the left insular gyri in participants (all in left, male in middle, and females in right columns, respectively).

Table 3. Left insula anterior–posterior fMRI organization with respect to PLG

		All				Male				Female			
Model details		ASG	MSG	PSG	ALG	ASG	MSG	PSG	ALG	ASG	MSG	PSG	ALG
Main model: group, time	Significance as χ^2	283.17	226.91	170.1	152.2	234.88	126.58	83.56	60.96	115.08	63.46	78.01	156.33
	< 0.001(all $p < 0.0001$)												
	Fit ($-2 \log$ -likelihood)	15 479.7	21 921.8	26 022.6	26 213.8	11 252.7	15 359.5	18 170.6	18 288.5	3855.9	4900.6	7183.8	7693.6
Group effect p -value (mean over entire series for each group)		0.84	0.3	0.55	0.82	0.25	0.69	0.77	0.91	0.02	0.24	0.25	0.81
Valsalva response: within- group		Time (within-group effect of time) p -values											
	Main	<0.001	<0.001	0.04	0.65	<0.001	0.02	0.1	0.27	<0.001	<0.001	<0.01	0.67
	Age	<0.001	<0.001	0.04	0.65	<0.001	0.02	0.1	0.27	<0.001	<0.001	<0.01	0.67
	Age \times Group	<0.001	<0.001	0.04	0.65	<0.001	0.02	0.1	0.27	<0.001	<0.001	<0.01	0.67
	Age \times Time	0.34	0.81	0.79	0.84	0.51	0.81	0.69	0.74	0.61	0.36	0.27	0.15
	Age \times Group \times Time	0.34	0.81	0.79	0.84	0.51	0.81	0.69	0.74	0.61	0.36	0.27	0.15
	HR	<0.001	<0.001	0.04	0.65	<0.001	0.02	0.09	0.27	<0.001	<0.001	<0.01	0.67
	HR \times Group	<0.001	<0.001	0.04	0.65	<0.001	0.02	0.1	0.27	<0.001	<0.001	<0.01	0.67
	HR \times Time	0.59	0.20	0.38	0.56	0.97	0.37	0.91	0.97	<0.001	<0.001	<0.01	0.24
	HR \times Group \times Time	0.59	0.20	0.38	0.56	0.97	0.37	0.91	0.97	<0.001	<0.001	<0.01	0.24
Valsalva response: between- group		Time \times Group (between-group effect of time) p -values											
	Main	0.44	0.15	0.16	0.11	0.02	0.24	0.19	0.08	0.04	0.87	0.67	0.47
	Age	0.44	0.15	0.16	0.11	0.02	0.24	0.19	0.09	0.04	0.87	0.67	0.47
	Age \times Group	0.44	0.15	0.16	0.11	0.02	0.24	0.19	0.09	0.04	0.87	0.67	0.47
	Age \times Time	0.46	0.16	0.17	0.11	0.02	0.24	0.19	0.09	0.03	0.82	0.60	0.36
	Age \times Group \times Time	0.46	0.16	0.17	0.11	0.02	0.24	0.19	0.09	0.03	0.82	0.60	0.36
	HR	0.44	0.15	0.16	0.11	0.02	0.24	0.19	0.08	0.04	0.87	0.67	0.47
	HR \times Group	0.44	0.15	0.16	0.11	0.03	0.24	0.19	0.08	0.04	0.87	0.67	0.47
	HR \times Time	0.44	0.15	0.16	0.11	0.03	0.30	0.24	0.13	0.45	0.32	0.26	0.44
	HR \times Group \times Time	0.44	0.15	0.16	0.11	0.03	0.30	0.24	0.13	0.45	0.32	0.26	0.44

The model fit is indicated by $-2 \times \log$ -likelihood as calculated by SAS (higher indicates better fit). The p -value variables in models are reported (italicized if ≤ 0.05). This table presents salient statistics from nine RMANOVA models for left insula anterior–posterior organization in three sets (mixed, male, female). Full data are available online [54]. The main model (bold) is the interaction of group-by-time (fMRI = group + time + group \times time), and measures of significance and fit are in the top rows of the table. The “Group” effect is the mean over the entire series and does not represent responses, and is not discussed. The two effects of interest “Time,” which represents within-group responses over time, and “Time \times Group,” which represents between-group differences in responses. The p -values for these effects are shown for the nine models. All models include the main effects plus additional mean or interaction terms. All interaction models also include means. For example, “Age \times Time” is fMRI = group + time + group \times time + age + age \times time.

in Table 5 show that no between-group differences appeared in the combined groups. Both OSA and control groups showed right dominance in the three posteriormost gyri (PSG, ALG, PLG). Males showed a modest OSA effect (reduced laterality compared with control) only in the PLG. Right dominance in male OSA and control groups was significance only in the PSG and ALG. Similarly, females showed no laterality differences between OSA and control occurred in any gyri. However, all gyri other than ASG both groups exhibited right dominance. Note that females exhibit visible, but nonsignificant differences from baseline and between OSA and control (e.g. ASG in Figure 5), but the higher SEM values (error bars) in the females reflect less confidence in the mean and hence a lack of significance at the $p \leq 0.05$ level. Age had no influence on any within- or between-group effects. The interaction of baseline HR and time (meaning HR influence on Valsalva responses) influenced within-group effects for all groups in the ASG and MSG, and between-group effects in females in the ASG and ALG.

The full model results, including averaged time trends as presented in the figures, are available in a data repository [54].

Discussion

Overview

Consistent with prior studies in healthy people, we showed functional organization along anterior–posterior gyri and

lateralization of gyri during an autonomic challenge during the phase II sympathetic activation period. Combining data from both sexes led to minimal differences between OSA and control, with most gyri showing similar response patterns in both groups. Partitioning data by sex revealed that males also had similar patterns to the control participants, whereas the small sample of OSA females showed substantially greater right and anterior dominance in signals. Most patterns of response were associated with resting HR, and in a few cases, with age. While the smaller OSA female sample size limits generalizability of those findings, the data support the importance of partitioning regional brain responses to cardiovascular challenges by sex. The findings suggest that, at least in males, insula function is not necessarily a major driver of differences that are present in OSA such as weaker cardiovascular and global cerebral blood flow responses previously shown [15, 48].

Increased anterior insular activity during the sympathetic phase of the Valsalva maneuver occurs in OSA and healthy groups, consistent with the established autonomic function of this subregion found in both human neuroimaging and animal lesion studies [26, 36, 55]. Since no direct projections exist from the insula to either the premotor sympathetic neurons in the region of the rostral ventrolateral medulla (RVLM) or directly to sympathetic preganglionic cells in the lateral horn of the spinal cord, the insula must alter autonomic output via at least one relay [22]. One such pathway from the insula to the RVLM is via the hypothalamus, more

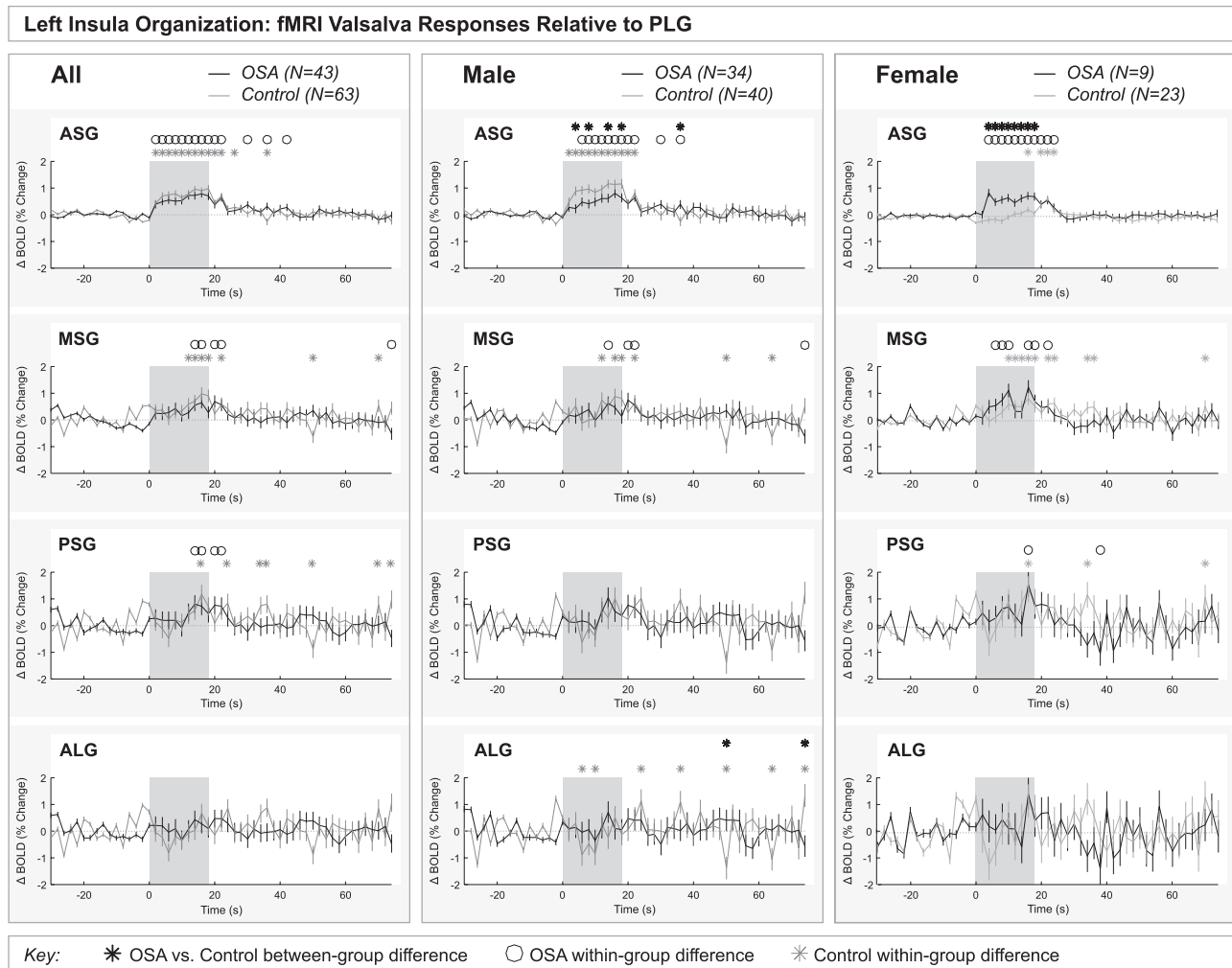


Figure 4. Anterior–posterior organization of right insula. Right hemisphere fMRI signals relative to PLG such that positive change reflects anterior dominance. Baseline (group mean \pm SE), averaged over four challenges, with time points of significant increase or decrease relative to baseline within-group, and time points of between-group differences (RMANOVA, $p \leq 0.05$) for the anterior–posterior responses by the right insular gyri in participants (all in left, male in middle, and females in right columns, respectively).

specifically from the agranular anterior insula, which encompasses the region displaying the greatest signal differences by sex during the Valsalva, and projects to multiple hypothalamic sites, including the ventromedial, dorsomedial, lateral, and posterior hypothalamus [56, 57]. Consistent with these anatomical projections, the insula, dorsomedial hypothalamus, ventromedial hypothalamus, and the RVLm display fMRI signal intensity changes coupled to resting bursts of muscle sympathetic activity, and these regions display ongoing signal covariation [20, 58, 59]. Additionally, stimulation of the anterior insula induces BP changes that are abolished by hypothalamic lesioning in animal studies [60]. Resting-state neuroimaging studies also revealed altered baseline function in insular cortices and altered functional connectivity from insula to other autonomic-related brain regions in OSA [61, 62]. Further, neurotransmitter levels differ in the insular cortices of OSA patients, with lower gamma aminobutyric acid (GABA) and higher glutamate [63]. Thus, altered resting levels of neural activity and functional coupling with ongoing sympathetic drive may be limiting or changing the responsiveness and organization of the insula in OSA.

Only limited evidence exists on neural function-related sex differences in OSA, but here we found that females specifically showed higher anterior signal dominance in both left and right insula during an autonomic challenge. However, relative to control participants, OSA males showed lower anterior dominance in the left insula and no difference in the right insula. Given previous resting-state and neurotransmitter findings of the insula in OSA, the question arises for future studies whether the baseline state is altered in a different manner in OSA females and males. The right insula is preferentially involved in sympathetic regulation, in contrast with more parasympathetic regulation on the left. Openheimer and colleagues [35] showed lateralization in insular cortex stimulation-elicited differential cardiovascular rhythm changes in epileptic patients, with right insula stimulation triggering sympathetic and left insula parasympathetic effects. Removal of the right insula in rats leads to increased parasympathetic activity [64]. Consistent with our study in healthy individuals [36], here we report that the direction of left–right organization is similar in both OSA and control groups, with higher activity on the right side. As with

Table 4. Right insula anterior–posterior fMRI organization with respect to PLG

Model details		All				Male				Female			
		ASG	MSG	PSG	ALG	ASG	MSG	PSG	ALG	ASG	MSG	PSG	ALG
Main model: group, time	Significance as $\chi^2 < 0.001$ (all $p < 0.0001$)	411.17	103.33	110.21	90.79	243.21	62.45	47.43	34.59	181.29	97.94	142.46	129.74
	Fit ($-2 \log$ -likelihood)	10 180.6	16 631.5	24 599.1	27 543.1	7529	11 783.9	17 241.5	19 257.8	2461.3	4756.6	7137.8	8027
	Group effect p -value (mean over entire series for each group)	0.39	0.82	0.92	0.81	0.4	0.92	0.58	0.63	0.02	0.65	0.23	0.71
Valsalva response: within- group	Time (within-group effect of time) p -values Main	<0.001	<0.001	<0.001	0.30	<0.001	<0.001	<0.01	0.14	<0.001	<0.001	<0.01	0.41
	Age	<0.001	<0.001	<0.001	0.30	<0.001	<0.001	<0.01	0.14	<0.001	<0.001	<0.01	0.41
	Age \times Group	<0.001	<0.001	<0.001	0.30	<0.001	<0.001	<0.01	0.14	<0.001	<0.001	<0.01	0.41
	Age \times Time	0.78	0.66	0.62	0.57	0.67	0.27	0.45	0.56	0.69	0.20	0.04	0.07
	Age \times Group \times Time	0.78	0.66	0.62	0.57	0.67	0.27	0.45	0.56	0.69	0.20	0.04	0.07
	HR	<0.001	<0.001	<0.001	0.30	<0.001	<0.001	<0.01	0.14	<0.001	<0.001	<0.01	0.41
	HR \times Group	<0.001	<0.001	<0.001	0.30	<0.001	<0.001	<0.01	0.14	<0.001	<0.001	<0.01	0.41
	HR \times Time	<0.001	0.02	0.23	0.27	0.047	0.23	0.91	0.94	<0.001	<0.01	0.03	0.047
	HR \times Group \times Time	<0.001	0.02	0.23	0.27	0.047	0.23	0.91	0.94	<0.001	<0.01	0.03	0.047
Valsalva response: between- group	Time \times Group (between-group effect of time) p -values Main	0.93	0.18	0.06	0.08	0.66	0.18	0.07	0.06	<0.001	0.09	0.38	0.45
	Age	0.93	0.18	0.06	0.08	0.66	0.18	0.07	0.06	<0.001	0.09	0.38	0.45
	Age \times Group	0.93	0.18	0.06	0.08	0.66	0.18	0.07	0.06	<0.001	0.09	0.38	0.45
	Age \times Time	0.91	0.17	0.06	0.08	0.65	0.17	0.07	0.06	<0.001	0.05	0.26	0.36
	Age \times Group \times Time	0.91	0.17	0.06	0.08	0.65	0.17	0.07	0.06	<0.001	0.05	0.26	0.36
	HR	0.93	0.18	0.06	0.08	0.66	0.18	0.07	0.06	<0.001	0.09	0.38	0.45
	HR \times Group	0.93	0.18	0.06	0.08	0.66	0.18	0.07	0.06	<0.001	0.09	0.38	0.45
	HR \times Time	0.94	0.18	0.06	0.08	0.71	0.24	0.09	0.08	<0.001	0.02	0.27	0.49
	HR \times Group \times Time	0.94	0.18	0.06	0.08	0.71	0.24	0.09	0.08	<0.001	0.02	0.27	0.49

The model fit is indicated by $-2 \times \log$ -likelihood as calculated by SAS (higher indicates better fit). The p -value variables in models are reported (italicized if ≤ 0.05). This table presents salient statistics from nine RMANOVA models for right insula anterior–posterior organization in three sets (mixed, male, female). Full data are available online [54]. The main model (bold) is the interaction of group-by-time (fMRI = group + time + group \times time), and measures of significance and fit are in the top rows of the table. The “Group” effect is the mean over the entire series and does not represent responses, and is not discussed. The two effects of interest “Time,” which represents within-group responses over time, and “Time \times Group,” which represents between-group differences in responses. The p -values for these effects are shown for the nine models. All models include the main effects plus additional mean or interaction terms. All interaction models also include means. For example, “Age \times Time” is fMRI = group + time + group \times time + age + age \times time.

anterior–posterior organization, again consistent with our previous findings in healthy control participants, the more anterior regions of the insula displayed greater signal intensity changes in both controls and OSA groups.

While there was similar magnitude of lateralization in control and grouped OSA participants, we found significant signal right dominance in females from both groups across all gyri. The altered lateralization could reflect differences from a common baseline, or limiting effects due to sex-specific baseline differences in neurotransmitter levels or functional state. Higher functional connectivity appears in the insula in females compared to males following visceral stimulation (noxious pain) in rats [65]. These organizational differences between females and males may be reflected in the sex differences in cardiovascular responses [38]. The autonomic changes during a Valsalva are well documented and elicit a standard sequence of BP and HR responses, which reflect the strength of the baroreflex and cerebral autoregulation [15, 46]. We previously showed that HR during the initial part of the Valsalva (phase II) in healthy females was higher than healthy males, along with healthy females showing higher cerebral blood flow fMRI response during Valsalva than healthy males [38]. In OSA females, the HR is lower than OSA males in this phase of Valsalva, but compared to respective controls, both males and females have lower HR in OSA versus control [15]. Our current findings in the insula fMRI responses may relate to the HR response during Valsalva

in that females show a more pronounced change than males [15]. Alternatively, females may need to exert greater proportional responses, since the target pressure was set at an absolute 30 mmHg, which presumably would require less effort for stronger individuals (and males are in the average stronger than females). It is therefore possible that a protocol based on a target pressure at a percentage of maximum would reveal similar responses between the sexes.

The question remains as to whether the OSA differences in insula organization reported here would be affected by treatments such as CPAP therapy. Muscle sympathetic nerve activity (MSNA), which is elevated in OSA at rest [66], is reduced and even normalized with 6 months of CPAP treatment [3, 12, 67]. This reduction of sympathetic tone is likely due to CPAP supporting the normalization of brainstem structure and function specifically in medullary raphe, rostral ventrolateral medulla, dorsolateral pons, and ventral midbrain [12]. However, in addition to “normalized” function in brainstem autonomic sites, CPAP therapy apparently alters the coupling between activity and spontaneous sympathetic nerve activity in the insula, and, in particular, the region of the anterior agranular insula in OSA participants [3]. Other studies show improved brain structure with CPAP [68–70], and although the insula has not been explored in detail, it is possible that there is a benefit of CPAP with respect to insula structure and function.

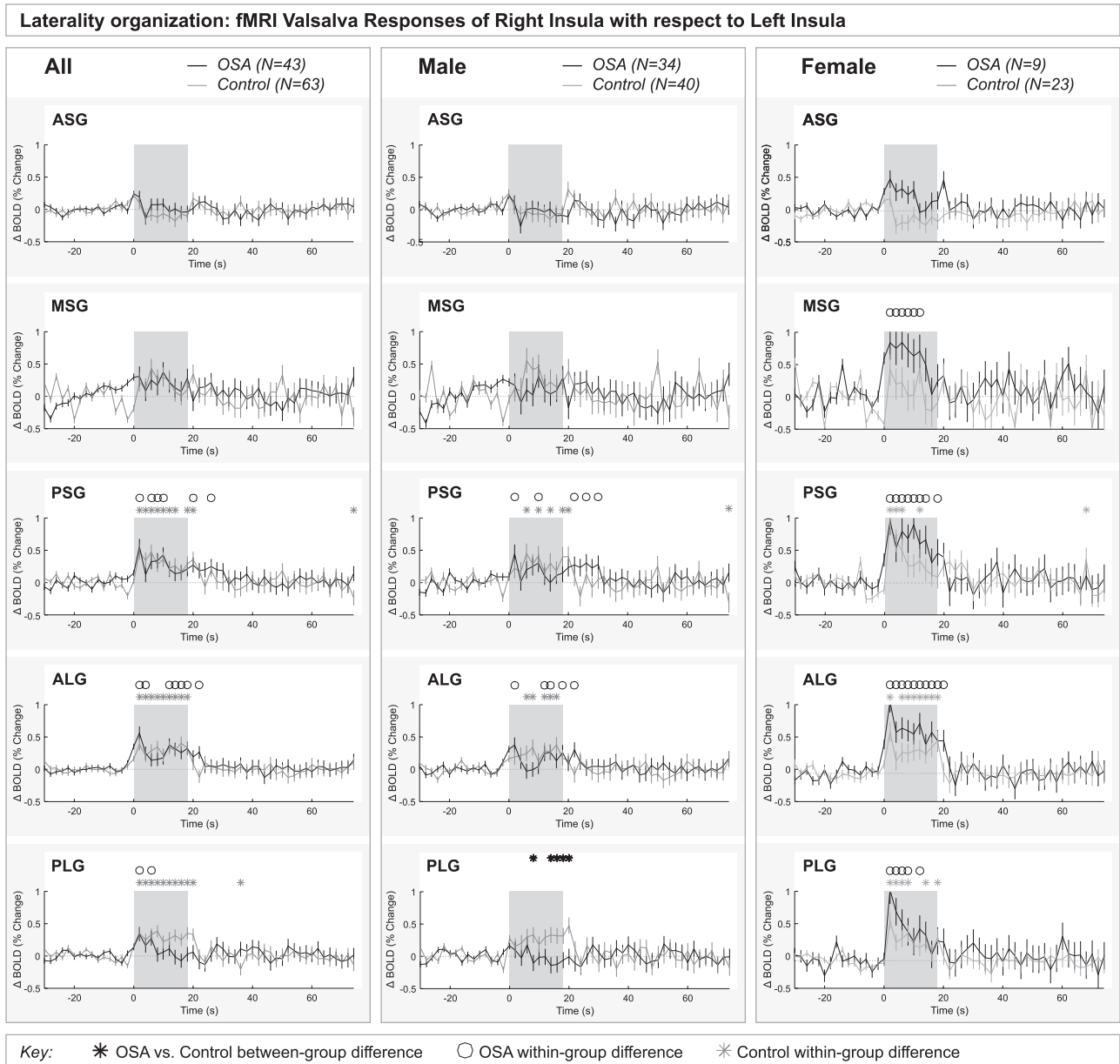


Figure 5. Lateralization by gyri. Right hemisphere fMRI signals relative to left hemisphere for all gyri (group mean \pm SE), averaged over four challenges, with time points of significant increase or decrease relative to baseline within-group, and time points of between-group differences (RMANOVA, $p \leq 0.05$) for the right-left laterality in insular gyri responses in participants (all in left, male in middle, and females in right columns, respectively).

Autonomic responsiveness changes with age [71, 72], which theoretically could be a factor in the present findings, since OSA is a progressive disease [73], and sex differences with aging influences may occur, given OSA is more common in postmenopausal women [74]. Nevertheless, the additional assessment of age, age-by-time, and age-by-group interactions revealed only limited influences. More specifically, the age-by-time interaction, meaning the response variation with age, affected some findings, whereas age-by-group interactions showed few effects. These secondary analyses therefore suggest that, even if cardiovascular responsiveness declines over time, age does not substantially affect functional organization of the insular in healthy or people with OSA.

Resting HR was closely associated with the fMRI response patterns, which reflects a close association between resting

state and extent of responses. A high starting HR likely means a lower HR response to the Valsalva, meaning a ceiling effect. As the fMRI signals reflect control of HR, albeit indirect, so a close relationship is not unexpected. Links between resting autonomic state and responsiveness may involve insular regulation, and could be worthy of further investigation, starting in a healthy population.

Obesity and endothelial dysfunction could also contribute to the findings since both are frequently comorbid with OSA [75]. Variability in individual anatomy could have led to variability in separation of insular gyri [76], but the fMRI signal is only sensitive to within a few millimeters [77]; thus, a finer anatomical distinction would be unlikely to make a noticeable difference in the findings. We had fewer females than males in our study, so while we did see substantial sex differences,

Table 5. Laterality of insular fMRI organization

		All					Male					Female				
Model details		ASG	MSG	PSG	ALG	PLG	ASG	MSG	PSG	ALG	PLG	ASG	MSG	PSG	ALG	PLG
Main model: group, time	Significance as $\chi^2 < 0.001$ (all $p < 0.0001$)	863.13	303.29	599.13	685.92	392.1	661.32	224.12	461.44	411.72	257.54	218.35	117.84	155.01	298.36	141.34
	Fit ($-2 \log$ -likelihood)	10 973.8	17 067.5	13 871.4	12 083.1	12 483.6	8111.8	12 083.3	9865.2	8402.3	8909.2	2769.5	4891	3961.4	3657	3554.6
	Group effect p -value (mean over entire series for each group)	0.75	0.54	0.7	0.73	0.55	0.77	0.77	0.73	0.92	0.25	0.07	0.03	0.57	0.34	0.31
Valsalva re- sponse: within-group	Time (within-group effect of time) p -values															
	Main	0.2	0.1	<0.001	<0.001	<0.001	0.74	0.51	<0.001	<0.01	0.32	0.49	<0.01	<0.001	<0.001	<0.001
	Age	0.21	0.11	<0.001	<0.001	<0.001	0.74	0.51	<0.001	<0.01	0.32	0.49	<0.01	<0.001	<0.001	<0.001
	Age \times Group	0.20	0.11	<0.001	<0.001	<0.001	0.74	0.51	<0.001	<0.01	0.32	0.49	<0.01	<0.001	<0.001	<0.001
	Age \times Time	0.99	0.95	0.99	0.40	0.83	0.62	0.91	0.96	0.99	0.046	<0.001	0.61	0.95	0.16	0.59
	Age \times Group \times Time	0.99	0.95	0.99	0.40	0.83	0.62	0.91	0.96	0.99	0.046	<0.001	0.61	0.95	0.16	0.59
	HR	0.20	0.11	<0.001	<0.001	<0.001	0.74	0.51	<0.001	<0.01	0.32	0.49	<0.01	<0.001	<0.001	<0.001
	HR \times Group	0.20	0.11	<0.001	<0.001	<0.001	0.74	0.51	<0.001	<0.01	0.32	0.49	<0.01	<0.001	<0.001	<0.001
	HR \times Time	0.04	0.22	<0.001	<0.001	0.18	0.95	0.20	<0.001	<0.001	0.41	<0.001	0.81	0.17	<0.001	0.47
	HR \times Group \times Time	0.04	0.22	<0.001	<0.001	0.18	0.95	0.20	<0.001	<0.001	0.41	<0.001	0.81	0.17	<0.001	0.47
Valsalva response: between- group	Time \times Group (between-group effect of time) p -values															
	Main	0.85	0.34	0.89	0.97	0.11	0.65	0.25	0.45	0.82	0.02	0.10	0.73	0.91	0.72	0.99
	Age	0.85	0.34	0.89	0.97	0.11	0.65	0.25	0.45	0.82	0.02	0.10	0.73	0.91	0.72	0.99
	Age \times Group	0.85	0.34	0.89	0.97	0.11	0.65	0.25	0.45	0.82	0.02	0.10	0.73	0.91	0.72	0.99
	Age \times Time	0.85	0.37	0.91	0.97	0.11	0.65	0.26	0.47	0.83	0.01	0.23	0.69	0.94	0.90	0.99
	Age \times Group \times Time	0.85	0.37	0.91	0.97	0.11	0.65	0.26	0.47	0.83	0.01	0.23	0.69	0.94	0.90	0.99
	HR	0.85	0.34	0.89	0.97	0.11	0.65	0.25	0.45	0.82	0.02	0.10	0.73	0.91	0.72	0.99
	HR \times Group	0.85	0.34	0.89	0.97	0.11	0.65	0.25	0.45	0.82	0.02	0.10	0.73	0.91	0.72	0.99
	HR \times Time	0.86	0.34	0.87	0.96	0.11	0.59	0.26	0.68	0.93	0.02	0.62	0.43	0.97	0.99	0.99
	HR \times Group \times Time	0.86	0.34	0.87	0.96	0.11	0.59	0.26	0.68	0.93	0.02	0.62	0.43	0.97	0.99	0.99

The model fit is indicated by $-2 \times \log$ -likelihood as calculated by SAS (higher indicates better fit). The p -value variables in models are reported (italicized if ≤ 0.05). This table presents salient statistics from nine RMANOVA models for right-minus-left insula organization in three sets (mixed, male, female). Full data are available online [54]. The main model (bold) is the interaction of group-by-time (fMRI = group + time + group \times time), and measures of significance and fit are in the top rows of the table. The "Group" effect is the mean over the entire series and does not represent responses, and is not discussed. The two effects of interest "Time," which represents within-group responses over time, and "Time \times Group," which represents between-group differences in responses. The p -values for these effects are shown for the nine models. All models include the main effects plus additional mean or interaction terms. All interaction models also include means. For example, "Age \times Time" is fMRI = group + time + group \times time + age + age \times time.

a larger study is needed to confidently generalize the female OSA findings.

We did not consider other possible functional roles of the insula, like saliency and internal experience related to sensory perception. Separate from autonomic regulation, the Valsalva involves responding to a cue, using breathing muscles, and processing visual feedback (to maintain the target pressure), and experiencing chest pressure and dysnea later in the phase II of challenge, with relief in phases II and IV. Although these other functions are likely reflected to some degree in the insula, the substantial cardiovascular changes elicited by the maneuver are likely to dominate the functional responses. Nevertheless, the findings should not be viewed as an exact measure of autonomic-only neural responses.

In conclusion, the functional organization of the insular cortex is not substantially altered during a sympathetic challenge in people with OSA, especially in males. Females may have higher anterior and right fMRI signal dominance in insula gyri compared with healthy people, but the sample was

too small to generalize with confidence. Questions remain regarding the resting-state functional activity and connectivity with other autonomic regions such as the hypothalamus and brainstem. Another question is whether these functional patterns change with treatment. Finally, given the widespread brain injury in OSA, it remains to be determined whether brain regions other than the insula contribute to the poor cardiovascular and cerebral blood flow responses to the Valsalva observed in OSA.

Acknowledgements

This research was supported by the National Institute of Nursing Research (NR-017435) and National Institute of Heart, Lung and Blood Institute (HL135562). The funders had no role in study design, data collection and analysis, decision to publish, or preparation of the manuscript.

Conflict of interest statement. None declared.

References

- Tietjens JR, et al. Obstructive sleep apnea in cardiovascular disease: a review of the literature and proposed multidisciplinary clinical management strategy. *J Am Heart Assoc.* 2019;**8**(1):e010440.
- Senaratna CV, et al. Prevalence of obstructive sleep apnea in the general population: a systematic review. *Sleep Med Rev.* 2017;**34**:70–81.
- Fatouleh RH, et al. Reversal of functional changes in the brain associated with obstructive sleep apnoea following 6 months of CPAP. *Neuroimage Clin.* 2015;**7**:799–806.
- McEvoy RD, et al.; SAVE Investigators and Coordinators. CPAP for prevention of cardiovascular events in obstructive sleep apnea. *N Engl J Med.* 2016;**375**(10):919–931.
- Javaheri S, et al. Continuous positive airway pressure adherence for prevention of major adverse cerebrovascular and cardiovascular events in obstructive sleep apnea. *Am J Respir Crit Care Med.* 2020;**201**(5):607–610.
- Lei Q, et al. Effects of continuous positive airway pressure on blood pressure in patients with resistant hypertension and obstructive sleep apnea: a systematic review and meta-analysis of six randomized controlled trials. *J Bras Pneumol.* 2017;**43**(5):373–379.
- Martínez-García MA, et al.; Spanish Sleep Network. Effect of CPAP on blood pressure in patients with obstructive sleep apnea and resistant hypertension: the HIPARCO randomized clinical trial. *JAMA.* 2013;**310**(22):2407–2415.
- Ryan S. Pro: should asymptomatic patients with moderate-to-severe OSA be treated? *Breathe (Sheff).* 2019;**15**(1):7–10.
- Vakulin A, et al. Con: should asymptomatic patients with moderate-to-severe OSA be treated? *Breathe (Sheff).* 2019;**15**(1):11–14.
- Drager LF, et al. Treatment of obstructive sleep apnoea as primary or secondary prevention of cardiovascular disease: where do we stand now? *Curr Opin Pulm Med.* 2018;**24**(6):537–542.
- Joyeux-Faure M, et al. Continuous positive airway pressure reduces night-time blood pressure and heart rate in patients with obstructive sleep apnea and resistant hypertension: the RHOOSAS randomized controlled trial. *Front Neurol.* 2018;**9**:318.
- Henderson LA, et al. Effects of 12 months continuous positive airway pressure on sympathetic activity related brainstem function and structure in obstructive sleep apnea. *Front Neurosci.* 2016;**10**:90.
- Macey PM, et al. Brain structural changes in obstructive sleep apnea. *Sleep.* 2008;**31**(7):967–977.
- Somers VK, et al. Sympathetic neural mechanisms in obstructive sleep apnea. *J Clin Invest.* 1995;**96**(4):1897–1904.
- Macey PM, et al. Heart rate responses to autonomic challenges in obstructive sleep apnea. *PLoS One.* 2013;**8**(10):e76631.
- Marrone O, et al. Blood-pressure variability in patients with obstructive sleep apnea: current perspectives. *Nat Sci Sleep.* 2018;**10**:229–242.
- Dampney RA. Functional organization of central pathways regulating the cardiovascular system. *Physiol Rev.* 1994;**74**(2):323–364.
- Benarroch EE. The central autonomic network: functional organization, dysfunction, and perspective. *Mayo Clin Proc.* 1993;**68**(10):988–1001.
- Kimmerly DS. A review of human neuroimaging investigations involved with central autonomic regulation of baroreflex-mediated cardiovascular control. *Auton Neurosci.* 2017;**207**:10–21.
- Macefield VG, et al. Identification of the human sympathetic connectome involved in blood pressure regulation. *Neuroimage.* 2019;**202**:116119.
- Saper CB, et al. Chapter 23 - central autonomic system. In: Paxinos G, ed. *The Rat Nervous System.* 4th ed. San Diego, CA: Academic Press; 2015: 629–673.
- Saper CB. Convergence of autonomic and limbic connections in the insular cortex of the rat. *J Comp Neurol.* 1982;**210**(2):163–173.
- Henderson LA, et al. Neural responses to intravenous serotonin revealed by functional magnetic resonance imaging. *J Appl Physiol (1985).* 2002;**92**(1):331–342.
- Henderson LA, et al. Functional magnetic resonance signal changes in neural structures to baroreceptor reflex activation. *J Appl Physiol (1985).* 2004;**96**(2):693–703.
- Rector DM, et al. Cerebellar fastigial nuclei activity during blood pressure challenges. *J Appl Physiol (1985).* 2006;**101**(2):549–555.
- Oppenheimer S, et al. The insular cortex and the regulation of cardiac function. *Compr Physiol.* 2016;**6**(2):1081–1133.
- Kimmerly DS, et al. Cortical regions associated with autonomic cardiovascular regulation during lower body negative pressure in humans. *J Physiol.* 2005;**569**(Pt 1):331–345.
- Henderson LA, et al. Obstructive sleep apnoea and hypertension: the role of the central nervous system. *Curr Hypertens Rep.* 2016;**18**(7):59.
- Macey PM, et al. Brain morphology associated with obstructive sleep apnea. *Am J Respir Crit Care Med.* 2002;**166**(10):1382–1387.
- Kang J, et al. Changes in insular cortex metabolites in patients with obstructive sleep apnea syndrome. *Neuroreport.* 2018;**29**(12):981–986.
- Tummala S, et al. Non-Gaussian diffusion imaging shows brain myelin and axonal changes in obstructive sleep apnea. *J Comput Assist Tomogr.* 2017;**41**(2):181–189.
- Yadav SK, et al. Insular cortex metabolite changes in obstructive sleep apnea. *Sleep.* 2014;**37**(5):951–958.
- Kumar R, et al. Altered global and regional brain mean diffusivity in patients with obstructive sleep apnea. *J Neurosci Res.* 2012;**90**(10):2043–2052.
- Bisogni V, et al. The sympathetic nervous system and catecholamines metabolism in obstructive sleep apnoea. *J Thorac Dis.* 2016;**8**(2):243–254 [(dedicated to) the International Conference: Clinical Update Sleep 2016].
- Oppenheimer SM, et al. Cardiovascular effects of human insular cortex stimulation. *Neurology.* 1992;**42**(9):1727–1732.
- Macey PM, et al. Differential responses of the insular cortex gyri to autonomic challenges. *Auton Neurosci.* 2012;**168**(1–2):72–81.
- Ghaziri J, et al. The corticocortical structural connectivity of the human insula. *Cereb Cortex.* 2017;**27**(2):1216–1228.
- Macey PM, et al. Sex differences in insular cortex gyri responses to the Valsalva maneuver. *Front Neurol.* 2016;**7**:87.
- Oppenheimer S. Cerebrogenic cardiac arrhythmias: cortical lateralization and clinical significance. *Clin Auton Res.* 2006;**16**(1):6–11.
- Oppenheimer SM, et al. Plasma and organ catecholamine levels following stimulation of the rat insular cortex. *Brain Res.* 1992;**569**(2):221–228.
- Macey PM, et al. Sex differences in insular cortex gyri responses to a brief static handgrip challenge. *Biol Sex Differ.* 2017;**8**:13.
- Macey PM, et al. Sex differences in white matter alterations accompanying obstructive sleep apnea. *Sleep.* 2012;**35**(12):1603–1613.

43. Macey PM, et al. Obstructive sleep apnea and cortical thickness in females and males. *PLoS One*. 2018;**13**(3):e0193854.
44. Macey PM, et al. Sex-specific hippocampus volume changes in obstructive sleep apnea. *Neuroimage Clin*. 2018;**20**:305–317.
45. Han SH, et al. The effect of high evening blood pressure on obstructive sleep apnea-related morning blood pressure elevation: does sex modify this interaction effect? *Sleep Breath*. 2019;**23**(4):1255–1263.
46. Porth CJ, et al. The Valsalva maneuver: mechanisms and clinical implications. *Heart Lung*. 1984;**13**(5):507–518.
47. Kalbfleisch JH, et al. Evaluation of the heart rate response to the Valsalva maneuver. *Am Heart J*. 1978;**95**(6):707–715.
48. Macey PM, et al. Global brain blood-oxygen level responses to autonomic challenges in obstructive sleep apnea. *PLoS One*. 2014;**9**(8):e105261.
49. American Academy of Sleep Medicine Task Force. Sleep-related breathing disorders in adults: recommendations for syndrome definition and measurement techniques in clinical research. The Report of an American Academy of Sleep Medicine Task Force. *Sleep*. 1999;**22**(5):667–689.
50. Ashburner J. A fast diffeomorphic image registration algorithm. *Neuroimage*. 2007;**38**(1):95–113.
51. Mai JK, et al. *Atlas of the Human Brain*. San Diego, CA: Elsevier Academic Press; 2004.
52. Macey PM, et al. Detecting variable responses in time-series using repeated measures ANOVA: application to physiologic challenges. *F1000Res*. 2016;**5**:563.
53. Littell RC, et al. *SAS System for Mixed Models*. Cary, NC: SAS Institute Inc.; 1996.
54. Macey P. Summary fMRI data from Valsalva maneuver in OSA and control groups with separation by sex. *Harvard Dataverse*; 2020.
55. Oppenheimer S, et al. The insular cortex and the regulation of cardiac function. *Compr Physiol*. 2016;**6**(2):1081–1133.
56. Cechetto DF, et al. Subcortical sites mediating sympathetic responses from insular cortex in rats. *Am J Physiol*. 1990;**258**(1 Pt 2):R245–R255.
57. Ongür D, et al. Prefrontal cortical projections to the hypothalamus in macaque monkeys. *J Comp Neurol*. 1998;**401**(4):480–505.
58. Macefield VG, et al. “Real-time” imaging of cortical and subcortical sites of cardiovascular control: concurrent recordings of sympathetic nerve activity and fMRI in awake subjects. *J Neurophysiol*. 2016;**116**(3):1199–1207.
59. Henderson LA, et al. Identification of sites of sympathetic outflow during concurrent recordings of sympathetic nerve activity and fMRI. *Anat Rec (Hoboken)*. 2012;**295**(9):1396–1403.
60. Wall PD, et al. Three cerebral cortical systems affecting autonomic function. *J Neurophysiol*. 1951;**14**(6):507–517.
61. Park B, et al. Aberrant insular functional network integrity in patients with obstructive sleep apnea. *Sleep*. 2016;**39**(5):989–1000.
62. Zhang Q, et al. Functional disconnection of the right anterior insula in obstructive sleep apnea. *Sleep Med*. 2015;**16**(9):1062–1070.
63. Macey PM, et al. Obstructive sleep apnea is associated with low GABA and high glutamate in the insular cortex. *J Sleep Res*. 2016;**25**(4):390–394.
64. de Morree HM, et al. Effects of insula resection on autonomic nervous system activity. *J Neurosurg Anesthesiol*. 2016;**28**(2):153–158.
65. Wang Z, et al. Sex differences in insular functional connectivity in response to noxious visceral stimulation in rats. *Brain Res*. 2019;**1717**:15–26.
66. Carlson JT, et al. Augmented resting sympathetic activity in awake patients with obstructive sleep apnea. *Chest*. 1993;**103**(6):1763–1768.
67. Waradekar NV, et al. Influence of treatment on muscle sympathetic nerve activity in sleep apnea. *Am J Respir Crit Care Med*. 1996;**153**(4 Pt 1):1333–1338.
68. Owen JE, et al. Neuropathological investigation of cell layer thickness and myelination in the hippocampus of people with obstructive sleep apnea. *Sleep*. 2019;**42**(1). doi:[10.1093/sleep/zsy199](https://doi.org/10.1093/sleep/zsy199)
69. Kim H, et al. Effects of long-term treatment on brain volume in patients with obstructive sleep apnea syndrome. *Hum Brain Mapp*. 2016;**37**(1):395–409.
70. Castronovo V, et al. White matter integrity in obstructive sleep apnea before and after treatment. *Sleep*. 2014;**37**(9):1465–1475.
71. Jensen-Urstad K, et al. Heart rate variability in healthy subjects is related to age and gender. *Acta Physiol Scand*. 1997;**160**(3):235–241.
72. Reardon M, et al. Changes in heart rate variability with age. *Pacing Clin Electrophysiol*. 1996;**19**(11 Pt 2):1863–1866.
73. Norman D, et al. Obstructive sleep apnea in older adults. *Clin Geriatr Med*. 2008;**24**(1):151–65, ix.
74. Huang T, et al. Type of menopause, age at menopause, and risk of developing obstructive sleep apnea in postmenopausal women. *Am J Epidemiol*. 2018;**187**(7):1370–1379.
75. Bonsignore MR, et al. Obstructive sleep apnea and comorbidities: a dangerous liaison. *Multidiscip Respir Med*. 2019;**14**:8.
76. Rosen A, et al. A neuroimaging strategy for the three-dimensional in vivo anatomical visualization and characterization of insular gyri. *Stereotact Funct Neurosurg*. 2015;**93**(4):255–264.
77. Olman CA, et al. High-field fMRI for human applications: an overview of spatial resolution and signal specificity. *Open Neuroimag J*. 2011;**5**:74–89.